Signal of four muons or more from a vector-like lepton decaying to a muon-philic Z' boson at the LHC

Junichiro Kawamura[1,2,*] and Stuart Raby[3,†]

[1]*Center for Theoretical Physics of the Universe, Institute for Basic Science (IBS), Daejeon 34051, Korea*
[2]*Department of Physics, Keio University, Yokohama 223-8522, Japan*
[3]*Department of Physics, Ohio State University, Columbus, Ohio, 43210, USA*

(Received 22 April 2021; accepted 15 July 2021; published 11 August 2021)

We propose a novel possibility to detect a very distinctive signal with more than four muons originating from pair-produced vector-like leptons decaying to a muon-philic Z' boson. These new particles are good candidates to explain the anomalies in the muon anomalous magnetic moment and the $b \to s\ell\ell$ processes. The doublet (singlet) vector-like leptons lighter than 1.3 (1.0) TeV are excluded by the latest data at the LHC if $\mathrm{BR}(E \to Z'\mu) = 1$. We also show that the excess in the signal region with more than five leptons can be explained by this scenario if the vector-like lepton is a weak singlet, with mass about 400 GeV and $\mathrm{BR}(E \to Z'\mu) = 0.25$. The future prospects at the HL-LHC are discussed.

DOI: 10.1103/PhysRevD.104.035007

I. INTRODUCTION

The Large Hadron Collider (LHC) explores new physics beyond the Standard Model (SM) at TeV-scale. The SM has been established as the theory just above the electroweak (EW) scale, particularly by the discovery of the 125 GeV Higgs boson at the LHC [1,2]. Although most of the experiments are consistent with the predictions of the SM, there are 2–3σ discrepancies in the measurements of rare semileptonic B meson decays [3–19], $b \to s\ell\ell$, and the 4.2σ discrepancy in the anomalous magnetic moment of muon, Δa_μ [20–42]. An interesting coincidence here is that both anomalies are found in physics related to muons, and hence these could be explained by the same origin. One way to establish these discrepancies as evidence of new physics is to increase the significance by reducing the uncertainties in the experimental measurements and in the predictions of the SM. Another way is by directly discovering new particles at the LHC, which we pursue in this paper.

It was shown in Refs. [43,44] that both anomalies in $b \to s\ell\ell$ and Δa_μ are addressed by introducing vector-like (VL) fermions and a Z' boson associated with an additional gauge symmetry $U(1)'$.[1] The former anomaly is explained by Z' exchange at the tree-level,[2] while the latter is explained by loop corrections involving the VL leptons and the Z' boson. In this paper, we point out the possibility that pair productions of VL leptons provide very distinctive signals with more than four muons. We shall discuss the current limits from the recent ATLAS data [69] and future prospects at the HL-LHC in a simplified model with a VL lepton and Z' boson. We also discuss the possible explanation for the excess in the more than 5-lepton signal found in Ref. [69].

The rest of this paper is organized as follows. The simplified model is defined and then the relation to the anomalies are discussed in Sec. II. In Sec. III, we discuss limits from the high-multiplicity lepton signal at the LHC. Section IV is devoted to summary. The model proposed in Refs. [43,44] are reviewed in the Appendix as a UV completion of the simplified model.

II. SIMPLIFIED MODEL

We shall consider the simplified model with a VL lepton E, which is weak singletlike, E_1, or doubletlike, $L = (E_2, N)$, where N is the $SU(2)_L$ partner of E_2. The Z' boson couplings to the leptons are given by

*jkawa@ibs.re.kr
†raby.1@osu.edu

[1]See Refs. [45–50] for models with VL fermions and $U(1)'$ for the anomalies. The VL lepton explanation for Δa_μ is studied in, e.g., Refs. [51–57]. See also Ref. [58] for roles of VL leptons to the EW-fit and the CKM matrix determination.

[2]The $b \to s\ell\ell$ anomaly can be explained by loop corrections involving VL families [59–68].

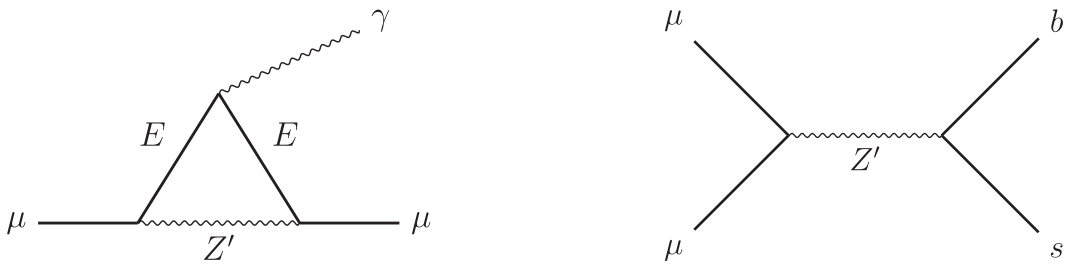

FIG. 1. Diagrams contribute to Δa_μ (left) and the $b \to s\ell\ell$ decay (right).

$$\mathcal{L}_{Z'} = Z'_\mu(\bar{\mu}\,\bar{E})\gamma^\mu\left[\begin{pmatrix} g^L_{\mu\mu} & g^L_{\mu E} \\ g^L_{\mu E} & g^L_{EE}\end{pmatrix}P_L + \begin{pmatrix} g^R_{\mu\mu} & g^R_{\mu E} \\ g^R_{\mu E} & g^R_{EE}\end{pmatrix}P_R\right]\begin{pmatrix}\mu \\ E\end{pmatrix} + Z'_\mu(\bar{\nu}\,\bar{N})\gamma^\mu\left[\begin{pmatrix} g^L_{\nu\nu} & g^L_{\nu N} \\ g^L_{\nu N} & g^L_{NN}\end{pmatrix}P_L + \begin{pmatrix} 0 & 0 \\ 0 & g^R_{NN}\end{pmatrix}P_R\right]\begin{pmatrix}\nu \\ N\end{pmatrix}, \tag{1}$$

where $E = E_1$ or E_2 and the interactions with N in the second line are absent in the case of weak singlet VL lepton. We assume that the off-diagonal couplings of the SM bosons to the SM and VL leptons are negligible, such that the dominant decay modes of the VL leptons are the decays to a Z' boson and SM lepton. In fact, this is achieved in the model proposed in Refs. [43,44].

The loop corrections involving the VL leptons and the Z' boson contribute to the anomalous magnetic moment of the muon. The diagram is shown in the left panel of Fig. 1. It is known that the chiral-flip effect should be sizable to explain the current discrepancy of $\mathcal{O}(10^{-9})$ with the new particles above the EW scale. In models with VL leptons, the chiral-flip effects may come from the nonzero VEV of the SM Higgs doublet. Hence the size of the loop correction is estimated as

$$\Delta a_\mu \sim -\frac{m_\mu \kappa v_H}{8\pi^2 m^2_{Z'}} g^L_{\mu E} g^R_{\mu E} C_{\Delta a_\mu} \sim 2.9\times 10^{-9}\times\left(\frac{500\ \text{GeV}}{m_{Z'}}\right)^2\left(\frac{\kappa}{0.5}\right)\left(\frac{\sqrt{g^L_{\mu E}g^R_{\mu E}}}{0.25}\right)^2\left(\frac{C_{\Delta a_\mu}}{0.1}\right), \tag{2}$$

where κ is the Yukawa couping constant for $\tilde{H}\bar{L}_R E_L$. $C_{\Delta a_\mu}$ is the factor from loop functions which is typically of $\mathcal{O}(0.1)$, see Appendix for the explicit form in the example model.

The Z' boson couplings to muons, $g^L_{\mu\mu}$ and $g^R_{\mu\mu}$, directly relate to the Wilson coefficients for the $b \to s\ell\ell$ decay. The diagram is shown in the right panel of Fig. 1. The effective Hamiltonian is given by [70,71]

$$\mathcal{H}_{\text{eff}} = -\frac{4G_F}{\sqrt{2}}\frac{\alpha_e}{4\pi}V_{tb}V^*_{ts}(C_9\mathcal{O}_9 + C_{10}\mathcal{O}_{10}), \tag{3}$$

where

$$\mathcal{O}_9 \coloneqq [\bar{s}\gamma^\mu P_L b][\bar{\mu}\gamma_\mu\mu], \qquad \mathcal{O}_{10} \coloneqq [\bar{s}\gamma^\mu P_L b][\bar{\mu}\gamma_\mu\gamma_5\mu]. \tag{4}$$

The coefficients in this model are given by [43,44]

$$C_9 = -\frac{\sqrt{2}}{4G_F}\frac{4\pi}{\alpha_e}\frac{1}{V_{tb}V^*_{ts}}\frac{g^L_{sb}}{2m^2_{Z'}}(g^R_{\mu\mu} + g^L_{\mu\mu}), \tag{5}$$

$$C_{10} = -\frac{\sqrt{2}}{4G_F}\frac{4\pi}{\alpha_e}\frac{1}{V_{tb}V^*_{ts}}\frac{g^L_{sb}}{2m^2_{Z'}}(g^R_{\mu\mu} - g^L_{\mu\mu}), \tag{6}$$

where g^L_{sb} is the Z' couplings to $\bar{s}b$ in the left-current. The value of C_9 is estimated as

$$|C_9| \sim 0.87\times\left(\frac{m_{Z'}}{500\ \text{GeV}}\right)^2\left(\frac{g^L_{sb}}{0.0007}\right)\left(\frac{g^L_{\mu\mu}+g^R_{\mu\mu}}{0.5}\right). \tag{7}$$

Note that the Z' couplings to quarks are tiny to explain the $b \to s\ell\ell$ anomaly, while those to muons are large so that Δa_μ is explained when $g^{L,R}_{\mu\mu} \sim g^{L,R}_{\mu E}$, which is true in the sample model. This feature ensures that the Z' mass of $\mathcal{O}(100\ \text{GeV})$ is not excluded by the dilepton resonance search at the LHC [72].[3] Although the flavor violating coupling with the quarks g^L_{sb} is tiny, the flavor conserving

[3]See Refs. [73,74] for general discussions for Z' boson responsible for $b \to s\ell\ell$.

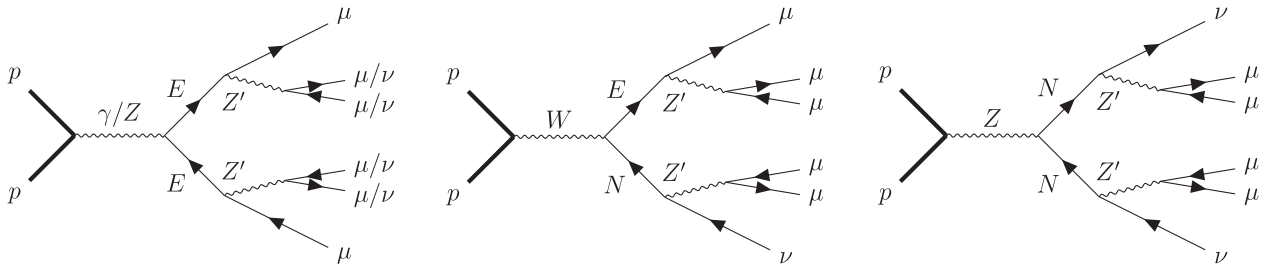

FIG. 2. Processes can produce more than four muons. The signal of more than four muons is produced if either of the Z' boson decays to a pair of muons from the charged VL lepton pair production (left), while both have to decay to muons in the other processes (middle and right) involving the VL neutrino.

couplings, e.g., g^L_{ss} or g^L_{bb}, can be sizable depending on a model, and thus the lower limit on the Z' boson can be much tighter. In other words, the Z' boson search provides a powerful tool to discriminate models for the anomalies. In the sample model shown in Appendix, however, the fiducial cross section can be less than $\mathcal{O}(1\ \mathrm{fb})$ which is much below the current limit as shown in Fig. 4 in Ref. [44].

In the Z' boson explanation, the ratio of the coefficients are given by

$$\frac{C_{10}}{C_9} = \frac{g^R_{\mu\mu} - g^L_{\mu\mu}}{g^R_{\mu\mu} + g^L_{\mu\mu}}. \tag{8}$$

The recent analyses [75–77] including the measurement of R_K based on the full run-2 data at the LHCb [19][4] favor C_9-only, C_{10}-only and $C_9 = -C_{10}$ scenarios among the one dimensional analyses, which correspond to $g^R_{\mu\mu} = g^L_{\mu\mu}$, $g^R_{\mu\mu} = -g^L_{\mu\mu}$ and $g^R_{\mu\mu} = 0$, respectively. Among these three cases, the explanation by $C_9 = -C_{10}$ is not preferred to explain the Δa_μ anomaly because $\Delta a_\mu \propto g^L_{\mu\mu} g^R_{\mu\mu}$, see Eq. (2). From this observation, we shall consider the case with $|g^L_{\mu\mu}| = |g^R_{\mu\mu}|$ which predicts

$$\begin{aligned}\mathrm{BR}(Z' \to \mu\mu) &\coloneqq \frac{\Gamma(Z' \to \mu\mu)}{\Gamma(Z' \to \nu\nu) + \Gamma(Z' \to \mu\mu)} \\ &\simeq \frac{|g^L_{\mu\mu}|^2 + |g^R_{\mu\mu}|^2}{2|g^L_{\mu\mu}|^2 + |g^R_{\mu\mu}|^2} = \frac{2}{3}.\end{aligned} \tag{9}$$

Here, we assume $g^L_{\mu\mu} = g^L_{\nu\nu}$ as expected from the $SU(2)_L$ symmetry and the Z' boson decay to quarks are negligible as expected from Eq. (7). Studies for $|g^L_{\mu\mu}| \neq |g^R_{\mu\mu}|$, as preferred by the two dimensional analyses on (C_9, C_{10}) plane, are interesting but are beyond the scope of this paper.

III. LHC SIGNALS

In this paper, we study signals from pair produced VL leptons decaying to the second generation leptons and the Z' boson. This can be realized when the VL leptons are heavier than the Z' boson. If the Z' boson is heavier, the VL lepton may decay to a SM boson and a lepton. The limits for VL leptons in such a case are studied in Refs. [95–101]. It is also possible that the VL lepton decays to a new boson, such as the physical mode of the $U(1)'$ breaking scalar. Thus we treat the branching fraction of $E/N \to Z'\mu/\nu$ as a free-parameter. We further assume $\mathrm{BR}(N \to Z'\nu) = \mathrm{BR}(E \to Z'\mu)$ for simplicity. Figure 2 shows the relevant processes which can generate signals for more than four muons.[5] Only the left process is relevant for the singlet-like case.

We recast the limits obtained in Refs. [69,104]. The former searches for signals with more than four leptons, and the latter searches for signals with exactly two leptons with large missing transverse energy, E_T^{miss}. We have generated events using MadGraph5_2_8_2 [105] based on a UFO [106] model file generated with FeynRules_2_3_43 [105,107]. The events are showered with PYTHIA8 [108] and then run through the fast detector simulator DELPHES3.4.2 [108]. We used the default ATLAS card for the detector simulation, but the threshold on p_T for the muon efficiency formula is changed to 5 GeV from 10 GeV since muons with $p_T > 5$ GeV are counted as signal muons in Ref. [69].

We recast the experimental limits on the signal regions without Z boson, b-jet and hadronic τ defined in Ref. [69].[6] These are named $\mathtt{SRO}^{\mathrm{loose}}_{\mathrm{bveto}}$, $\mathtt{SRO}^{\mathrm{tight}}_{\mathrm{bveto}}$ and SR5L. The requirements for the events, in addition to the b-jet veto and hadronic τ-veto, common in the signal regions are as follows. To meet the trigger thresholds, p_T of the leading muon, ordered by p_T, must be larger than 27 GeV, or p_T's of the leading and next-to leading muons are required to be larger than (15,15) GeV or (23,9) GeV. If an opposite-sign (OS) muon pair whose invariant mass m_{OS} is less than 4 GeV or $8.4 < m_{\mathrm{OS}} < 10.4$ GeV, both leptons are discarded. If two muons are found in $\Delta R < 0.6$ and one of them has $p_T < 30$ GeV, both leptons are discarded. The first (second) Z candidate is found from a pair of OS muons

[4]See Refs. [78–94] for the analyses before the Moriond 2021.

[5]We used TikZ-FeynHand to draw these figures [102,103].

[6]We recast the analysis such that light leptons, (e, μ), in Ref. [69], for our simple model these are just muons.

TABLE I. The number of events observed (data), fitted SM backgrounds (SM) and 95% C.L. upper bound on the number of signal events (S^{95}) in the signal regions [69,104].

	$\mathtt{SRO}^{\mathrm{loose}}_{\mathrm{bveto}}$	$\mathtt{SRO}^{\mathrm{tight}}_{\mathrm{bveto}}$	SR5L	SR2L
data	11	1	21	37
SM	$11.5^{+2.9}_{-2.2}$	$3.5^{+2.0}_{-2.2}$	12.4 ± 2.3	37.3 ± 3.0
S^{95}	9.79	3.87	17.88	14.3

whose m_{OS} is the (second) closest to the Z boson mass $m_Z = 91.2$ GeV. A pair is identified as a Z boson if $m_{\mathrm{OS}} \in [81.2, 101.2]$ GeV. Further, the event is considered to have a Z boson if any system of $\mu^+\mu^-\mu^\pm$ or $\mu^+\mu^-\mu^+\mu^-$ has invariant mass in [81.1, 101.2] GeV. In the signal regions $\mathtt{SRO}^{\mathrm{loose}}_{\mathrm{bveto}}$ and $\mathtt{SRO}^{\mathrm{tight}}_{\mathrm{bveto}}$, there must be more than four muons after the selections above, and the event must not have any combinations of muons which is identified as a Z boson. Further, the effective mass of the event m_{eff}, defined as the scalar sum of E_T^{miss}, p_T of signal leptons and p_T of the jets with $p_T > 40$ GeV, is required to be larger than 600 (1250) GeV in the $\mathtt{SRO}^{\mathrm{loose}}_{\mathrm{bveto}}$ ($\mathtt{SRO}^{\mathrm{tight}}_{\mathrm{bveto}}$). In the SR5L, the requirement is simply the lepton number to be larger than five, and no further selection applied.

We also study the limits from the SUSY slepton search [104] which requires exactly two leptons and large E_T^{miss}. The most relevant signal region for our scenario is with same flavor (SF) two leptons without any jet. There must be exactly two OSSF leptons, both with $p_T > 25$ GeV. Events are rejected if there are more muons with $p_T > 10$ GeV and $|\eta| < 2.7$ or the two leading leptons are not opposite sign. The missing energy E_T^{miss} and invariant mass of two leptons m_{OS} must be larger than 110 GeV and 121.2 GeV, respectively. The stransverse mass m_{T2} [109,110] is required to be larger than 160 GeV.[7] We name this signal region as SR2L.

The number of observed events, fitted SM backgrounds and 95% C.L. upper bounds on the signal events in the signal regions are shown in Table I. We see that there is an excess over the SM background in SR5L for which the local significance is 1.9σ. Figure 3 shows the production cross sections of VL leptons at $\sqrt{s} = 13$ TeV and 14 TeV calculated by MadGraph5. We calculated the probability of how many events pass the cuts in each signal region from the VL lepton pair production at $\sqrt{s} = 13$ TeV by generating 25000 (50000) events at each point on the $(m_E, m_{Z'})$ plane for the singletlike (doubletlike) VL leptons.

A. Current limits

Figures 4 and 5 show upper bounds on $\mathrm{BR}(E \to Z'\mu)$ in the signal regions, where the signal cross section is proportional to the branching fraction squared. In the gray region, $m_{Z'} > m_E$ and hence the decay $E \to Z'\mu$ is kinematically forbidden. The white region is not excluded by the current data even if $\mathrm{BR}(E \to Z'\mu) = 1$.

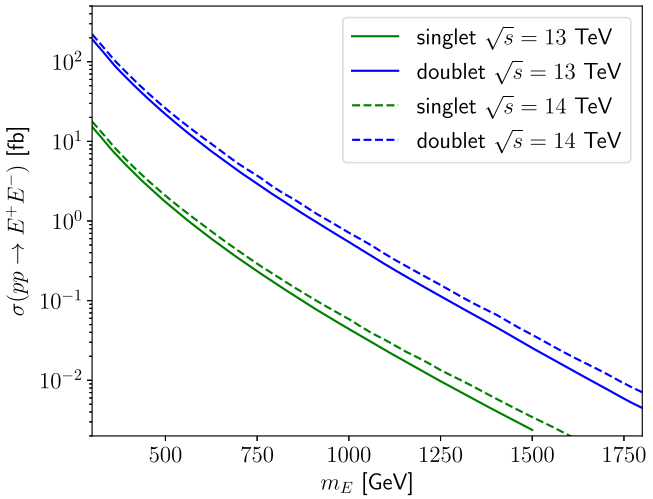

FIG. 3. Pair-production cross section of VL leptons at $\sqrt{s} = 13$ and 14 TeV. The productions of VL neutrinos are included in the doublet case.

For the doubletlike VL lepton, we see that $\mathtt{SRO}^{\mathrm{tight}}_{\mathrm{bveto}}$ gives the strongest bound if $\mathrm{BR}(E \to Z'\mu) \gtrsim 0.2$, because of fewer backgrounds satisfying the tighter m_{eff} cut. The current limit is about 1350 GeV if $\mathrm{BR}(E \to Z'\mu) = 1$. If the branching fraction is smaller, then $\mathtt{SRO}^{\mathrm{loose}}_{\mathrm{bveto}}$ gives the stronger bound, since the cut by $m_{\mathrm{eff}} > 1250$ GeV of the $\mathtt{SRO}^{\mathrm{tight}}_{\mathrm{bveto}}$ is too tight for $m_{E_2} \lesssim 600$ GeV. The limit from SR5L is weaker because of the excess and that from SR2L is also weaker due to the larger backgrounds. Note that the limits do not change much as the mass difference between the Z' boson and VL lepton decreases since the signal muons can originate from Z' decays.

For the singletlike VL lepton, the strongest bound of about 1000 GeV is again from the $\mathtt{SRO}^{\mathrm{tight}}_{\mathrm{bveto}}$ if $\mathrm{BR}(E \to Z'\mu) = 1$. The $\mathtt{SRO}^{\mathrm{tight}}_{\mathrm{bveto}}$ is not sensitive to the cases when $\mathrm{BR}(E \to Z'\mu) \lesssim 0.3$. The difference comes from smaller production cross section of the singletlike case. The $\mathtt{SRO}^{\mathrm{loose}}_{\mathrm{bveto}}$ gives the strongest constraint for smaller branching fractions. The limits from SR5L and SR2L are not shown, since the limits are much weaker than those from $\mathtt{SRO}^{\mathrm{tight}}_{\mathrm{bveto}}$ and $\mathtt{SRO}^{\mathrm{loose}}_{\mathrm{bveto}}$ for the same reason as the doubletlike case. In particular, SR2L gives no bounds for the singletlike case.

B. Explanation for the excess in SR5L

Figure 6 shows the upper bound on the number of signal events in the SR5L allowed by the limits from the other signal regions. The background colors represent maximum values of $\mathrm{BR}(E \to Z'\mu)$. Since the limits from the four

[7] We used the code provided by Ref. [111] to calculate the stransverse mass.

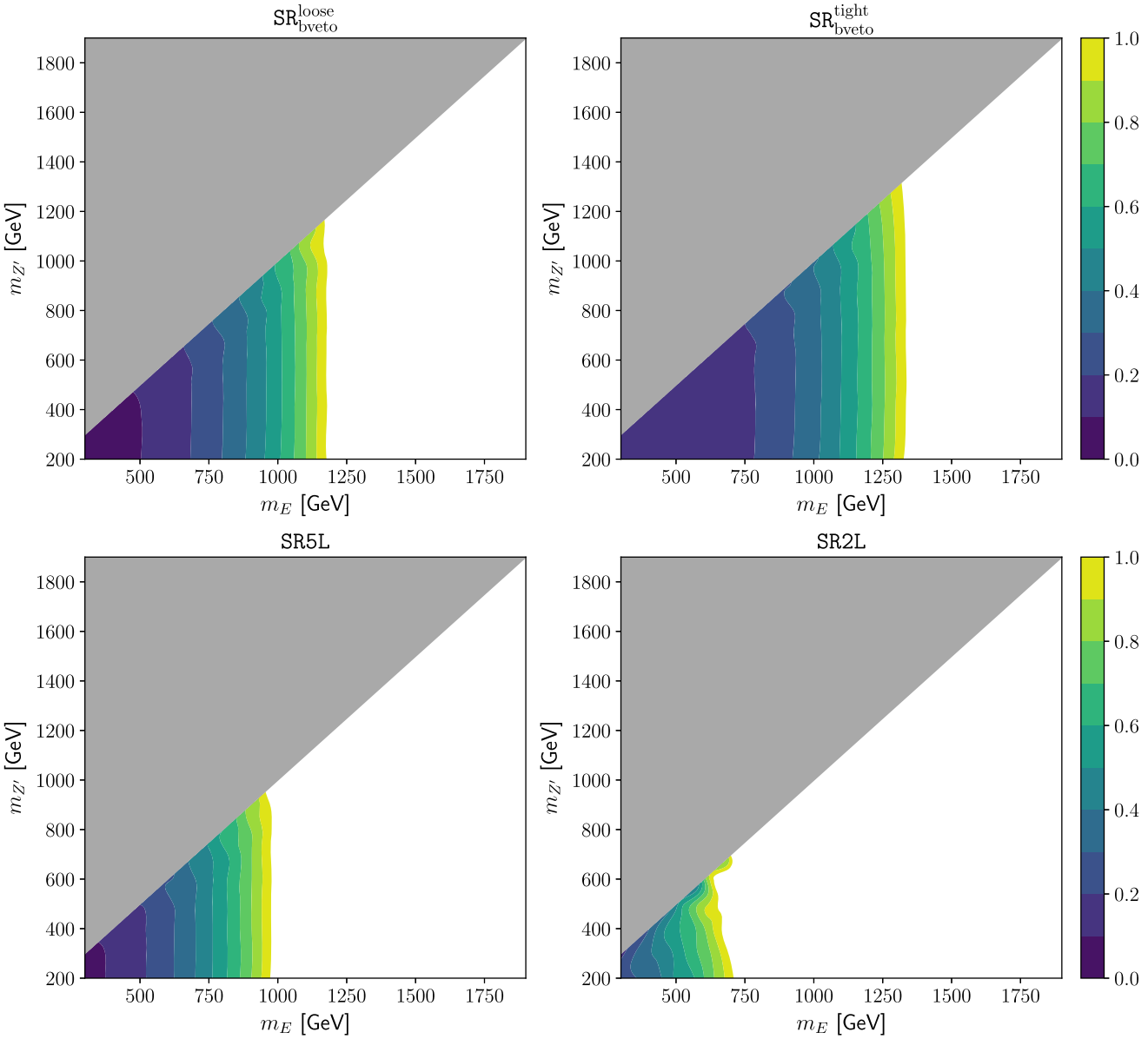

FIG. 4. Limits on BR$(E \to Z'\mu)$ for the doubletlike VL lepton.

lepton signal regions are severe, the branching fraction should be so small that the limits from $\texttt{SRO}^{\text{tight}}_{\text{bveto}}$ and $\texttt{SRO}^{\text{loose}}_{\text{bveto}}$ are relaxed by the fewer events passing the m_{eff} cut. The excess is explained on the solid green line when the SM background is at the central value shown in Table. I. The yellow band corresponds to the uncertainty of the background estimation. The singletlike VL lepton can more easily explain the excess. The limits from $\texttt{SRO}^{\text{tight}}_{\text{bveto}}$ and $\texttt{SRO}^{\text{loose}}_{\text{bveto}}$ are much stronger for the doubletlike case, since the production cross section is larger and there are fewer muon signals originating from the VL neutrino production.

The left panel of Fig. 7 shows the E_T^{miss} distribution after the selection of SR5L at the benchmark point with $m_{Z'} = 390$ GeV, $m_{E_1} = 400$ GeV and BR$(E_1 \to Z'\mu) = 0.25$. The SM contributions are represented by yellow bars and the black dots (bars) show the data (its error bar), which are read from Fig. 8 of Ref. [69]. We see that the E_T^{miss} distribution is well described by our scenario. The benchmark

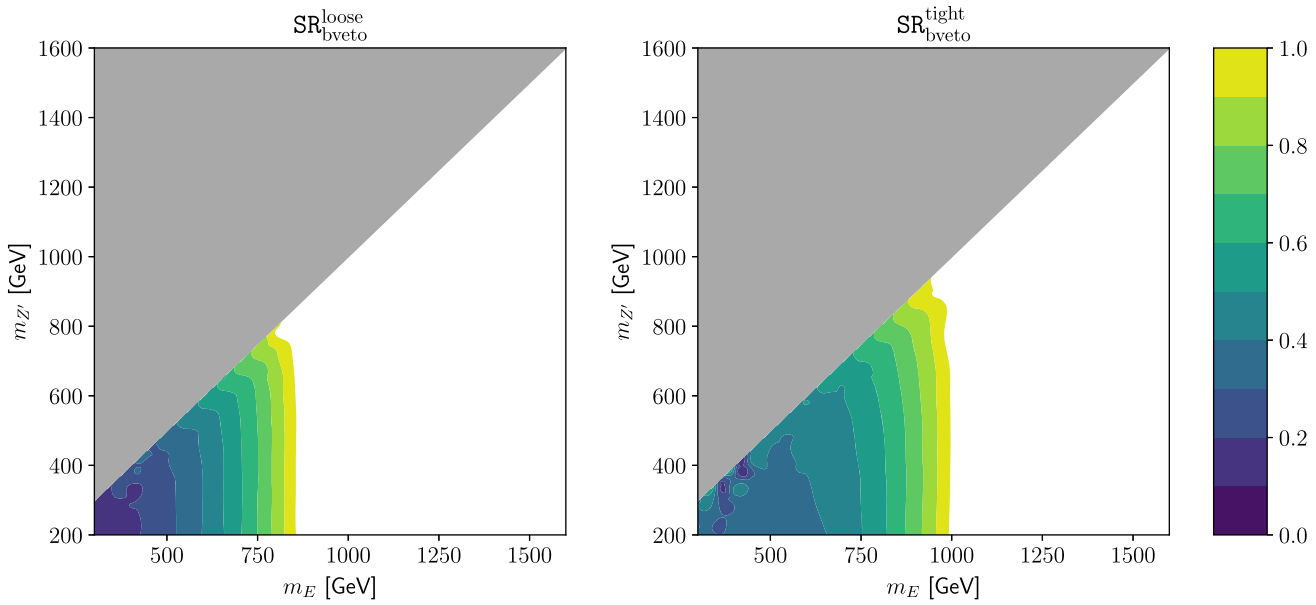

FIG. 5. Limits on $\mathrm{BR}(E \to Z'\mu)$ for the singletlike VL lepton.

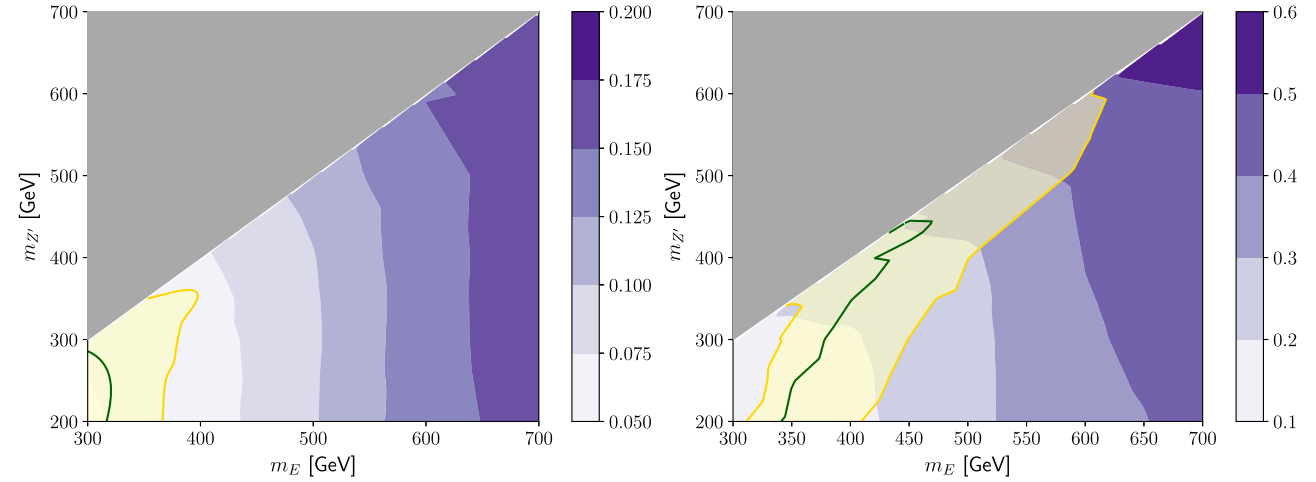

FIG. 6. Maximum values of the number of signal events in SR5L consistent with the limits of $\mathrm{SRO}^{\mathrm{loose}}_{\mathrm{bveto}}$ and $\mathrm{SRO}^{\mathrm{tight}}_{\mathrm{bveto}}$ for the doubletlike (singletlike) VL lepton in the left (right) panel. Background colors are the $\mathrm{BR}(E \to Z'\mu)$.

point in our example model which realizes these masses and branching fractions and is also consistent with the muon anomalies at the same time is shown Appendix A 3. The right panel of Fig. 7 shows the m_{eff} distribution after the selection of the number of muons to be larger than four. The values of the bars are normalized such that the sum of all the bins is unity. The green bars are for the same benchmark point as the left panel, and the red hatched bars are for another benchmark point with $m_{Z'} = 400$ GeV and $m_{E_1} = 1000$ GeV. We see that the peak of the distribution in m_{eff} is about $2m_{E_1}$, and hence the strong constraint from $\mathrm{SRO}^{\mathrm{tight}}_{\mathrm{bveto}}$, which requires $m_{\mathrm{eff}} > 1250$ GeV, is avoided and the tightest bound of $\mathrm{BR}(E \to Z'\mu) \lesssim 0.25$ is from $\mathrm{SRO}^{\mathrm{loose}}_{\mathrm{bveto}}$.

We emphasize that this model can only explain the SR5L excess by muons. Thus the SR5L excess cannot be explained, in this scenario, if it includes signals with

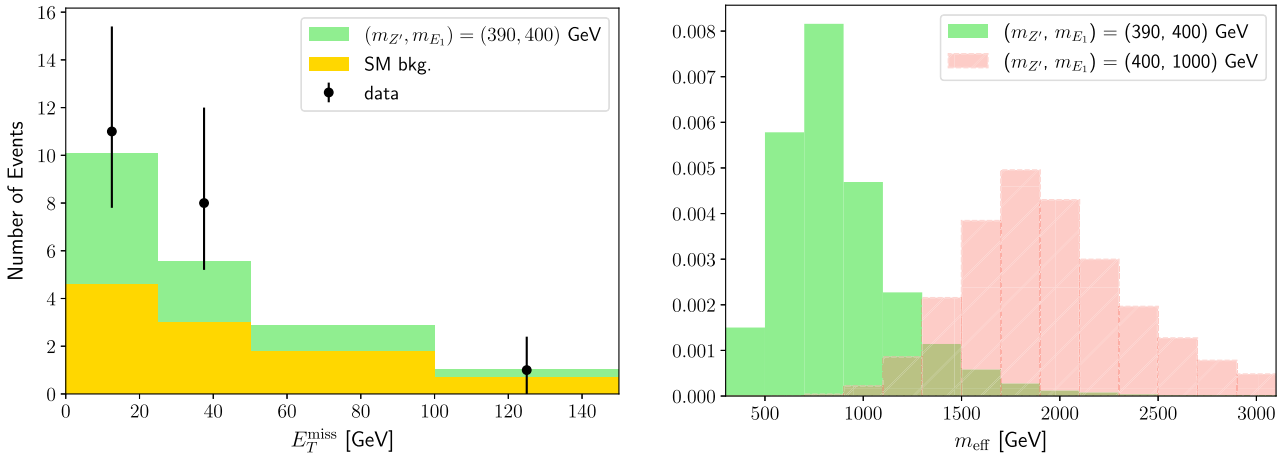

FIG. 7. Histograms of $E_T^{\rm miss}$ (left) and $m_{\rm eff}$ (right). In the left panel, $(m_{Z'}, m_{E_1}) = (390, 400)$ GeV and $\mathrm{BR}(E \to Z'\mu) = 0.25$. In the right panel, the values are normalized such that the total of the bins is unity.

electrons. The limits from the data would be significantly tightened if lepton flavors are specified in the signal regions. Thus the information of lepton flavor is crucial to test this model with a muon-philic Z' and VL leptons.

The excess with electrons, might be explained by VL leptons decaying to Z or W boson, where the SM bosons decay leptonically. If $m_{Z'} > m_{E_1}$ which is the opposite case to our scenario, the VL lepton will decay to a SM boson, including the Higgs boson. In addition, electrons may come from the decays of the heavier VL leptons, such as $E_2 \to E_1 Z$. We note that the roughly degenerate mass of the VL leptons are favored to explain the sizable Δa_μ in the model [44]. These possibilities are interesting, but beyond the scope of this paper.

C. Future prospects

We shall discuss the discovery and exclusion potential at the HL-LHC with 3 ab^{-1} data. We consider the two signal regions, $\mathtt{SRO}^{\rm tight}_{\rm bveto}$ and SR5L and propose two more new signal regions, SRZp and SR5L$'$.

We rescale the backgrounds to $\mathtt{SRO}^{\rm tight}_{\rm bveto}$ and SR5L by simply multiplying the ratio of integrated luminosity, 3000/139. For the signal events, we use the same efficiency times acceptance factor as those used in the analyses for the current limits. These are then multiplied by the integrated luminosity and the production cross section at $\sqrt{s} =$ 14 TeV shown in Fig. 3 to calculate the number of signal events.

We define the two new signal regions, named SRZp and SR5L$'$. In the SRZp, at least four muons are required and the Z-veto is applied. Then, two Z' candidates are chosen from any OS pair of muons, where the reference Z' mass, $m_{Z'}^{\rm ref}$, is set at 500 GeV, in the same manner as the Z candidates. The (next-to) leading Z' candidate, $m_{\rm OS}$ is the (second) closest to $m_{Z'}^{\rm ref}$, must satisfy $|m_{\rm OS} - m_{Z'}^{\rm ref}| < 100$ (250) GeV. We take relatively large range for the selection, because we do not know the Z' mass. The sensitivity can be improved by requiring strict range for $|m_{\rm OS} - m_{Z'}^{\rm ref}|$ and scan over $m_{Z'}^{\rm ref}$ in the analysis, as in the Z' searches [72,112]. In the SR5L$'$, more than 5 muons are required. Then, the Z-veto for any OS pair of muons and $m_{\rm eff} >$ 1000 GeV cuts are applied. In these two signal regions, we assume that there are 10 SM background events per 3 ab^{-1} data. This may be a conservative assumption, since the cut is very tight and not so many background events will survive, c.f. the rescaled backgrounds in $\mathtt{SRO}^{\rm tight}_{\rm bveto}$ and SR5L are 76.6 and 272, respectively.

We quantify the future discovery and exclusion limits by the p-values proposed in Ref. [113],

$$p_{\rm disc} = \frac{\gamma(s+b, b)}{\Gamma(s+b)}, \qquad p_{\rm excl} = \frac{\Gamma(b+1, s+b)}{\Gamma(b+1)}, \tag{10}$$

where s and b are the number of signals and backgrounds. $\Gamma(z)$, $\gamma(a,z)$ and $\Gamma(a,z)$ are the ordinary, lower incomplete and upper complete Gamma functions. The discovery (exclusion) limit corresponds to $p_{\rm disc} < 2.867 \times 10^{-7}$ ($p_{\rm excl} < 0.05$) where the significance is > 5 (> 1.645). Here, we do not consider uncertainties in the signals and backgrounds for simplicity.

The future prospects at the HL-LHC for the doublet-like and the singletlike VL leptons are shown in Fig. 8

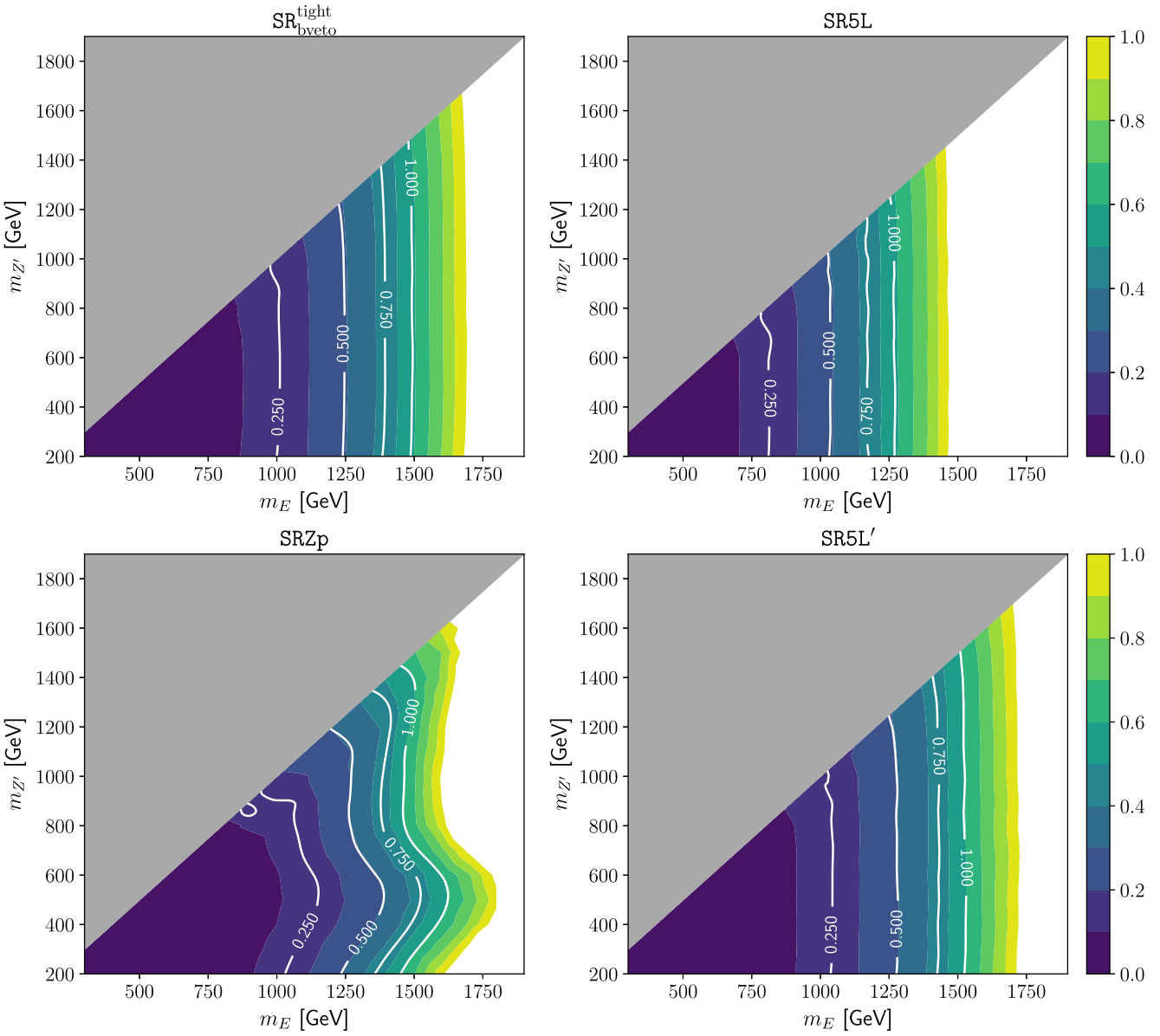

FIG. 8. Future prospects of the upper bound on $\mathrm{BR}(E \to Z'\mu)$ for the doubletlike VL lepton at the HL-LHC.

and 9, respectively. The background colors are the exclusion limits ($p_{\text{excl}} < 0.05$) for the branching fraction $\mathrm{BR}(E \to Z'\mu)$. The white lines show the discovery potential for a given branching fraction as labeled on the lines ($p_{\text{disc}} < 2.867 \times 10^{-7}$). Assuming $\mathrm{BR}(E \to Z'\mu) = 1$, the doubletlike (singletlike) VL lepton will be discovered up to $m_E \lesssim 1.5$ (1.15) TeV by $\mathtt{SRO}^{\text{tight}}_{\text{bveto}}$. The limits from SR5L are weaker. The SRZp may cover a wider parameter range than that of $\mathtt{SRO}^{\text{tight}}_{\text{bveto}}$ at $m_{Z'} \sim 500$ GeV even if we set the relatively large range for $|m_{\text{OS}} - m^{\text{ref}}_{Z'}|$. The SR5L′ may also cover a wider parameter range independent of the Z' mass, based on our assumption of the background. It is interesting that the entire parameter range with $\mathrm{BR}(E \to Z'\mu) \sim 0.25$, which can explain the excess in SR5L, can be discovered in SR5L, SRZp and SR5L′.

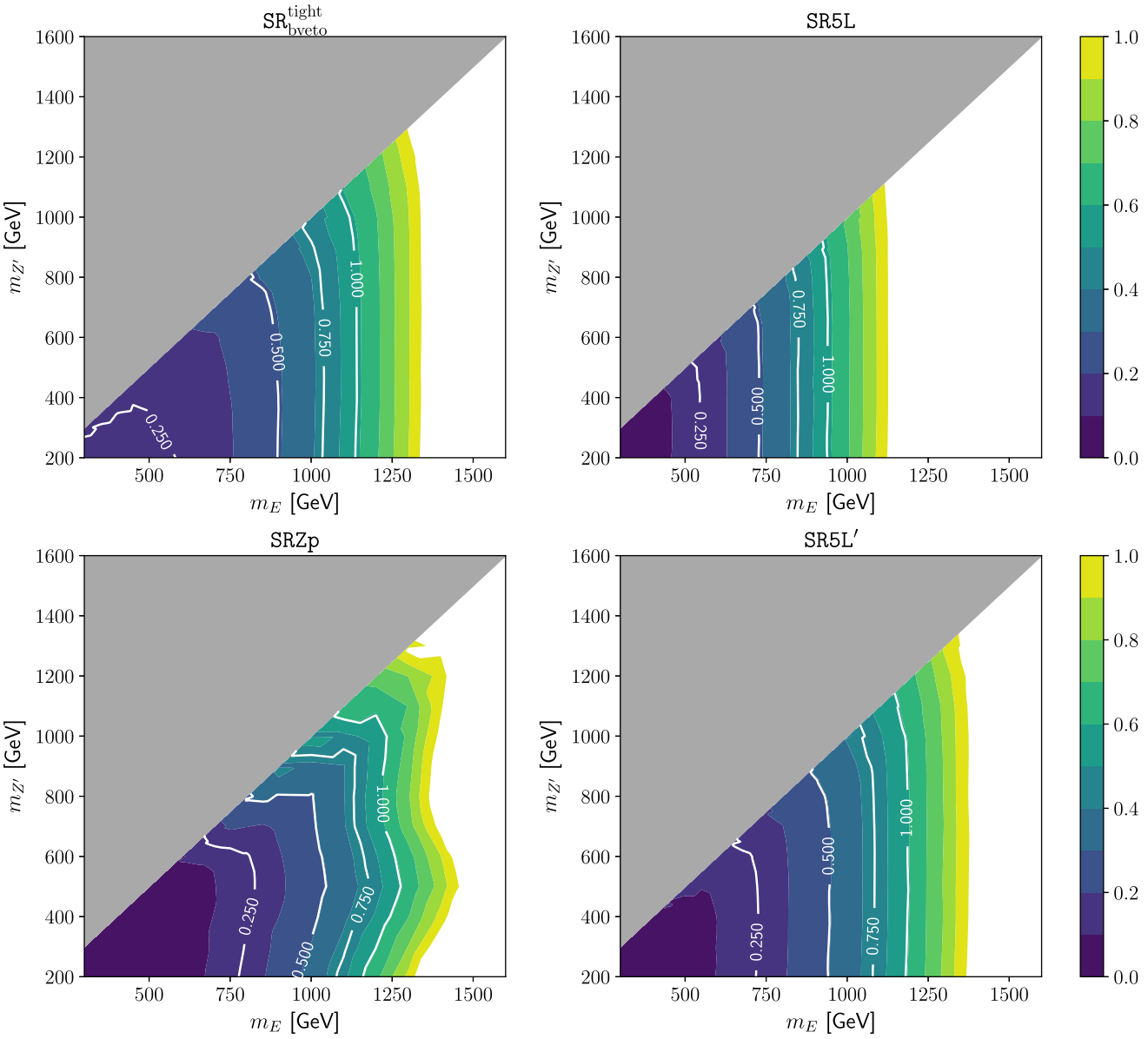

FIG. 9. Future prospects of the upper bound on BR$(E \to Z'\mu)$ for the singletlike VL lepton at the HL-LHC.

IV. DISCUSSIONS

In this paper, we study the signal with more than four muons originating from the pair-production of VL leptons decaying to a Z' boson which couples to muons and/or muon neutrinos. These particles may provide a way to resolve the tensions in the $b \to s\ell\ell$ decays and Δa_μ. The current limits can reach about 1 TeV when the VL lepton decays to the Z' boson exclusively owing to the very low backgrounds. We showed that the excess in the signal region with five leptons or more may be explained in our model if the excess is given *only by muons*. A benchmark point in our example model is given in Appendix A 3 which simultaneously explains the muon anomalies as well as the excess in SR5L. If the excess is not only muons, then the cascade decay of the heavier VL lepton might be a nice candidate to explain the excess with electrons and muons in this kind of model. The information of lepton flavor is crucial to test these new physics models which explain the muon anomalies.

ACKNOWLEDGMENTS

The work of J. K. is supported in part by the Institute for Basic Science (IBS-R018-D1), and the Grant-in-Aid for Scientific Research from the Ministry of Education, Science, Sports and Culture (MEXT), Japan No. 18K13534. The work of S. R. is supported in part by the Department of Energy (DOE) under Award No. DE-SC0011726.

Note added.—While finalizing this manuscript, the new experimental data of the muon anomalous magnetic moment was announced from the FNAL. The discrepancy from the SM prediction reaches to 4.2σ [22]. Models with VL leptons and a Z' boson coupling to muons nicely explains the discrepancy of Δa_μ, as well as the anomalies in $b \to s\ell\ell$. These new particles could be confirmed by the LHC as discussed in this paper.

APPENDIX: REVIEW OF VECTOR-LIKE $U(1)'$ MODEL

In this Appendix, we review the model proposed in Refs. [43,44] as an example of a UV completion of the simplified model. The matter contents of our model is given by Table II. The $SU(2)_L$ doublets are defined as

$$\ell_L = (\nu_L, \mu_L), \qquad H = (H_0, H_-),$$
$$L_L = (N'_L, E'_L), \qquad \bar{L}_R = (-\bar{E}'_R, \bar{N}'_R). \tag{A1}$$

We only consider muons, and assume that the couplings with the other leptons are negligible for simplicity. The masses of VL states and Yukawa interactions are given by

$$\mathcal{L} \supset -m_L \bar{L}_R L_L - m_E \bar{E}_R E_L + y_\mu \bar{\mu}_R \ell_L H + \kappa' \bar{E}_R L_L H - \kappa \bar{L}_R \tilde{H} E_L + \lambda_L \Phi \bar{L}_R \ell_L - \lambda_E \Phi \bar{\mu}_R E_L + \text{H.c.}, \tag{A2}$$

where $\tilde{H} \coloneqq i\sigma_2 H^* = (H^*_-, -H^*_0)$. The $SU(2)_L$ indices are contracted via $i\sigma_2$. After the symmetry breaking by $v_H \coloneqq \langle H_0 \rangle$ and $v_\Phi \coloneqq \langle \Phi \rangle$, the mass matrix for the leptons are given by

$$\bar{\mathbf{e}}_R \mathcal{M}_e \mathbf{e}_L \coloneqq \begin{pmatrix} \bar{\mu}_R & \bar{E}_R & \bar{E}'_R \end{pmatrix} \times \begin{pmatrix} y_\mu v_H & 0 & \lambda_E v_\Phi \\ 0 & \kappa' v_H & m_E \\ \lambda_L v_\Phi & m_L & \kappa v_H \end{pmatrix} \begin{pmatrix} \mu_L \\ E'_L \\ E_L \end{pmatrix}, \tag{A3}$$

$$\bar{\mathbf{n}}_R \mathcal{M}_n \mathbf{n}_L \coloneqq \bar{N}'_R \begin{pmatrix} \lambda_L v_\Phi & m_L \end{pmatrix} \begin{pmatrix} \nu_L \\ N'_L \end{pmatrix}. \tag{A4}$$

The mass basis is defined as

$$\hat{\mathbf{e}}_L \coloneqq U_L^\dagger \mathbf{e}_L, \quad \hat{\mathbf{e}}_R \coloneqq U_R^\dagger \mathbf{e}_R, \quad \hat{\mathbf{n}}_L \coloneqq V_L^\dagger \mathbf{n}_L, \quad \hat{\mathbf{n}}_R \coloneqq \mathbf{n}_R, \tag{A5}$$

TABLE II. Matter contents. Electric charge of fermion f is $Q_f = T^3_f + Y_f/2$.

	ℓ_L	$\bar{\mu}_R$	H	L_L	$\bar{E}_R$	$\bar{L}_R$	E_L	Z'	Φ
$SU(2)_L$	**2**	**1**	**2**	**2**	**1**	**2**	**1**	**1**	**1**
$U(1)_Y$	−1	2	−1	−1	2	1	−2	0	0
$U(1)'$	0	0	0	−1	1	1	−1	0	−1

where unitary matrices diagonalize the mass matrices as

$$U_R^\dagger \mathcal{M}_e U_L = \text{diag}(m_\mu, m_{E_2}, m_{E_1}), \quad \mathcal{M}_n V_L = \begin{pmatrix} 0 & m_N \end{pmatrix}, \tag{A6}$$

where E_1 (E_2) is the singletlike (doubletlike) VL lepton.[8] The nonzero mass of the SM neutrino will be explained by introducing the right-handed counterparts, but these are irrelevant for the present discussion.

We define the Dirac fermions as

$$\mathbf{e} \coloneqq (\mu, E_2, E_1), \qquad \mathbf{n} \coloneqq (\nu, N), \tag{A7}$$

where

$$[\mathbf{e}]_i \coloneqq ([\hat{\mathbf{e}}_L]_i, [\hat{\mathbf{e}}_R]_i), \quad \nu \coloneqq ([\hat{\mathbf{n}}_L]_1, 0), \quad N \coloneqq ([\hat{\mathbf{n}}_L]_2, N'_R), \tag{A8}$$

with $i = 1, 2, 3$.

1. Interactions

The gauge interactions with the Z' boson in the mass basis are defined as

$$\mathcal{L}_V = Z'_\mu \sum_{f=\mathbf{e},\mathbf{n}} \bar{f} \gamma^\mu (g^{Z'}_{f_L} P_L + g^{Z'}_{f_R} P_R) f, \tag{A9}$$

where the coupling matrices are given by

$$g^{Z'}_{\mathbf{e}_L} = g' U_L^\dagger Q'_e U_L, \qquad g^{Z'}_{\mathbf{e}_R} = g' U_R^\dagger Q'_e U_R,$$
$$g^{Z'}_{\mathbf{n}_L} = g' V_L^\dagger Q'_n V_L, \qquad g^{Z'}_{\mathbf{n}_R} = g' Q'_n. \tag{A10}$$

P_L (P_R) are the chiral projections onto the left- (right-) handed fermions. g' is the gauge coupling constant for $U(1)'$.

We expand the neutral scalar fields as

$$H_0 = v_H + \frac{1}{\sqrt{2}}(h + i a_h), \qquad \Phi = v_\Phi + \frac{1}{\sqrt{2}}(\chi + i a_\chi), \tag{A11}$$

where h and χ are the physical real scalar fields, while the pseudoscalar components a_h and a_χ are absorbed by the Z and Z' bosons, respectively. The Yukawa interactions are given by

$$-\mathcal{L}_Y = \frac{1}{\sqrt{2}} \sum_{S=h,\chi} \sum_{f=\mathbf{e},\mathbf{n}} S \bar{f} Y^S_f P_L f + \text{H.c.}, \tag{A12}$$

where

[8] We restrict cases which $m_{E_1} \ll m_{E_2}$ or $m_{E_1} \gg m_{E_2}$, so we can always identify the VL lepton is singletlike or doubletlike.

$$Y^h_{\mathbf{e}} = U_R^\dagger \begin{pmatrix} y_\mu & 0 & 0 \\ 0 & \kappa' & 0 \\ 0 & 0 & \kappa \end{pmatrix} U_L, \qquad Y^\chi_{\mathbf{e}} = U_R^\dagger \begin{pmatrix} 0 & 0 & \lambda_E \\ 0 & 0 & 0 \\ \lambda_L & 0 & 0 \end{pmatrix} U_L, \qquad Y^h_{\mathbf{n}} = 0_{2\times 2}, \qquad Y^\chi_{\mathbf{n}} = \begin{pmatrix} 0 & 0 \\ \lambda_L & 0 \end{pmatrix} V_L. \tag{A13}$$

Let us define the approximate masses of the VL leptons as

$$M_L \coloneqq \sqrt{m_L^2 + \lambda_L^2 v_\Phi^2}, \qquad M_E \coloneqq \sqrt{m_E^2 + \lambda_E^2 v_\Phi^2}. \tag{A14}$$

Assuming $\kappa v_H \ll |M_L - M_E|$, the diagonalization matrices for the charged lepton mass matrix are given by

$$U_L \sim \begin{pmatrix} c_L & s_L & -\delta_L s_L \\ -s_L & c_L & -\delta_L c_L \\ 0 & \delta_L & 1 \end{pmatrix} + \mathcal{O}(\delta_L^2), \qquad U_R \sim \begin{pmatrix} c_R & s_R\delta_R & s_R \\ -s_R & c_R\delta_R & c_R \\ 0 & 1 & -\delta_R \end{pmatrix} + \mathcal{O}(\delta_R^2), \tag{A15}$$

where

$$c_L \coloneqq \frac{m_L}{M_L}, \qquad s_L \coloneqq \frac{\lambda_L v_\Phi}{M_L}, \qquad \delta_L \coloneqq \frac{\kappa v_H M_L}{M_L^2 - M_E^2}, \tag{A16}$$

$$c_R \coloneqq \frac{m_E}{M_E}, \qquad s_R \coloneqq \frac{\lambda_E v_\Phi}{M_E}, \qquad \delta_R \coloneqq \frac{\kappa v_H M_E}{M_L^2 - M_E^2}. \tag{A17}$$

The diagonalized mass matrix is given by

$$U_R^\dagger \mathcal{M}_e U_L = \begin{pmatrix} (y_\mu c_L c_R + \kappa' s_L s_R) v_H & \mathcal{O}(m_\mu) & 0 \\ 0 & M_L + \mathcal{O}(\kappa v_H \delta_{L,R}) & 0 \\ \mathcal{O}(m_\mu) & \mathcal{O}(\kappa v_H \delta_{L,R}^2) & M_E + \mathcal{O}(\kappa v_H \delta_{L,R}) \end{pmatrix} + \mathcal{O}(m_\mu \delta_{L,R}), \tag{A18}$$

where we assume $y_\mu v_H, \kappa' v_H \lesssim m_\mu$ to explain the muon mass without fine-tuning.

The Z' couplings in the mass basis are approximately given by

$$g^{Z'}_{\mathbf{e}_L} = -g' \begin{pmatrix} s_L^2 & -c_L s_L & c_L s_L \delta_L \\ -c_L s_L & c_L^2 & s_L^2 \delta_L \\ c_L s_L \delta_L & s_L^2 \delta_L & 1 \end{pmatrix} + \mathcal{O}(\delta_L^2), \tag{A19}$$

$$g^{Z'}_{\mathbf{e}_R} = -g' \begin{pmatrix} s_R^2 & -c_R s_R \delta_R & -c_R s_R \\ -c_R s_R \delta_R & 1 & -s_R^2 \delta_R \\ -c_R s_R & -s_R^2 \delta_R & c_R^2 \end{pmatrix} + \mathcal{O}(\delta_R^2). \tag{A20}$$

Hence, the effective couplings defined in Eq. (1) are given by

$$\begin{pmatrix} g^L_{\mu\mu} & g^L_{\mu E} \\ g^L_{\mu E} & g^L_{EE} \end{pmatrix} \sim -g' \begin{pmatrix} s_L^2 & -s_L c_L \\ -s_L c_L & c_L^2 \end{pmatrix}, \qquad \begin{pmatrix} g^R_{\mu\mu} & g^R_{\mu E} \\ g^R_{\mu E} & g^R_{EE} \end{pmatrix} \sim -g' \begin{pmatrix} s_R^2 & -c_R s_R \delta_R \\ -c_R s_R \delta_R & 1 \end{pmatrix}, \tag{A21}$$

in the doubletlike case, and these are given by

$$\begin{pmatrix} g^L_{\mu\mu} & g^L_{\mu E} \\ g^L_{\mu E} & g^L_{EE} \end{pmatrix} \sim -g' \begin{pmatrix} s_L^2 & c_L s_L \delta_L \\ c_L s_L \delta_L & 1 \end{pmatrix}, \qquad \begin{pmatrix} g^R_{\mu\mu} & g^R_{\mu E} \\ g^R_{\mu E} & g^R_{EE} \end{pmatrix} \sim -g' \begin{pmatrix} s_R^2 & -c_R s_R \\ -c_R s_R & c_R^2 \end{pmatrix}, \tag{A22}$$

in the singletlike case.

The Yukawa couplings with χ are given by

$$Y^{\chi}_{\mathbf{e}} \sim \begin{pmatrix} 0 & \lambda_E c_R \delta_L & \lambda_E c_R \\ \lambda_L c_L & \lambda_L s_L & \lambda_E s_R \delta_R - \lambda_L s_L \delta_L \\ -\lambda_L c_L \delta_R & \lambda_E s_R \delta_L - \lambda_L s_L \delta_R & \lambda_E s_R \end{pmatrix}, \qquad Y^{\chi}_{\mathbf{n}} \sim \lambda_L \begin{pmatrix} 0 & 0 \\ c_L & s_L \end{pmatrix}, \tag{A23}$$

where the coupling of χ with $\mu\mu$ is as small as m_μ/m_E. The couplings to the SM bosons are the SM-like up to $\mathcal{O}(m_\mu/m_E)$.

2. Muon anomalies

The Z' and χ boson contribution to Δa_μ is given by [53,114]

$$\Delta a_\mu \sim \frac{m_\mu \kappa v_H}{64\pi^2 v_\Phi^2} s_{2L} s_{2R} C_{LR}, \tag{A24}$$

with

$$C_{LR} \coloneqq \sqrt{x_L x_E}\frac{G_Z(x_L) - G_Z(x_E)}{x_L - x_E} + \frac{1}{2}\sqrt{y_L y_R}\frac{y_L G_S(y_L) - y_R G_S(y_R)}{y_L - y_R}, \tag{A25}$$

where $x_L \coloneqq M_L^2/m_{Z'}^2$, $x_E \coloneqq M_E^2/m_{Z'}^2$, $y_L \coloneqq M_L^2/m_\chi^2$ and $y_E \coloneqq M_E^2/m_\chi^2$. Here, $m_{Z'}^2 = 2g'^2 v_\Phi^2$ is used. The loop functions are given by

$$G_Z(x) \coloneqq \frac{x^3 + 3x - 6x\ln(x) - 4}{2(1-x)^3}, \qquad G_S(y) \coloneqq \frac{y^2 - 4y + 2\ln(y) + 3}{(1-y)^3}. \tag{A26}$$

The contribution from the scalar χ is included since it is sizable unless m_χ is very heavy which requires very large quartic couplings.

For the $b \to s\mu\mu$ anomaly, the Wilson coefficients are given by

$$C_9 \sim -\frac{\sqrt{2}}{4G_F}\frac{4\pi}{\alpha_e}\frac{1}{V_{tb}V_{ts}^*}\frac{1}{4v_\Phi^2}(s_R^2 + s_L^2)\epsilon_{Q_e}\epsilon_{Q_3}, \tag{A27}$$

$$C_{10} \sim -\frac{\sqrt{2}}{4G_F}\frac{4\pi}{\alpha_e}\frac{1}{V_{tb}V_{ts}^*}\frac{1}{4v_\Phi^2}(s_R^2 - s_L^2)\epsilon_{Q_e}\epsilon_{Q_3}, \tag{A28}$$

where the Z' boson couplings to the SM doublet quarks are parametrized as

$$[g^{Z'}_{d_L}]_{ij} \sim [g^{Z'}_{u_L}]_{ij} \sim -g'\epsilon_{Q_i}\epsilon_{Q_j}. \tag{A29}$$

ϵ_{Q_i} is the similar quantity as $s_L \coloneqq \lambda_L v_\Phi/m_L$ and originates from the mixing between the SM and VL quarks, but we now consider the couplings with the second and third generation quarks and these are typically small in contrast to that for muon.

From Eq. (A24),

$$\Delta a_\mu \sim 2.9 \times 10^{-9} \times \left(\frac{1.0\ \text{TeV}}{v_\Phi}\right)^2 \left(\frac{\kappa}{1.0}\right)\left(\frac{s_{2L}s_{2R}}{1.0}\right)\left(\frac{C_{LR}}{0.1}\right). \tag{A30}$$

For the $b \to s\mu\mu$ anomaly,

$$C_9 \sim -0.62 \times \left(\frac{1.0\ \text{TeV}}{v_\Phi}\right)^2 \left(\frac{s_L^2 + s_R^2}{1}\right)\left(\frac{\epsilon_{Q_2}\epsilon_{Q_3}}{-0.002}\right). \tag{A31}$$

Assuming $s_L = s_R = 1/\sqrt{2}$, i.e., $\lambda_L v_\Phi = m_L$ and $\lambda_E v_\Phi = m_E$, the quark mixing angles are given by

$$\epsilon_{Q_2}\epsilon_{Q_3} \sim -0.003 \times \left(\frac{C_9}{-0.82}\right)\left(\frac{2.51\times 10^{-9}}{\Delta a_\mu}\right)\left(\frac{\kappa}{1.0}\right)\left(\frac{C_{LR}}{0.1}\right), \tag{A32}$$

when the both anomalies are explained. With such small couplings with quarks, Z' boson is sufficiently suppressed to be consistent with the constraints from the resonant dilepton signal search at the LHC [72], unless $\epsilon_{Q_2} \sim 1$ or $\epsilon_{Q_3} \sim 1$ to have large production cross section from $s\bar{s}$ or $b\bar{b}$, respectively. In fact, the fiducial cross section of $pp \to Z' \to \mu\mu$ can be less than $\mathcal{O}(1\ \text{fb})$ as shown in Fig. 4 in Ref. [44]. We also showed that the flavor violating coupling to bs is sufficiently small to be consistent with the mass difference of the B_s meson, ΔM_s, as well as the other related flavor observables [44].

3. Benchmark

We show a benchmark scenario which explains the anomalies in Δa_μ and $b \to s\ell\ell$ and the excess in SR5L simultaneously. As discussed in the main text, singletlike VL lepton is more suitable to explain the excess in SR5L. We take[9]

[9]With these values, $v_\Phi = 1103$ GeV which is sufficiently large to evade the bound from the neutrino trident process [115–120].

$$m_{Z'} = 390\ \text{GeV}, \quad M_L = 1.1\ \text{TeV}, \quad M_E = 404\ \text{GeV}, \quad m_\chi = 365\ \text{GeV},$$
$$s_L = s_R = 1/\sqrt{2}, \quad y_\mu v_H = 2m_\mu, \quad \kappa' = 0, \quad \kappa = -0.821, \quad g' = 0.25. \tag{A33}$$

The VL lepton masses are 400 and 1111 GeV. The correction to the anomalous magnetic moment of the muon is $\Delta a_\mu = 2.51 \times 10^{-9}$. $s_L = s_R$ realizes the C_9-only scenario, and $C_9 \sim -0.81$ is explained if $\epsilon_{Q_2}\epsilon_{Q_3} \sim -0.0032$.

The partial decay widths of the singlet VL lepton E_1 are approximately given by

$$\Gamma(E_1 \to Z'\mu) \sim \frac{M_E^3}{64\pi v_\Phi^2} c_R^2 s_R^2 (1-z)^2(1+2z), \tag{A34}$$

$$\Gamma(E_1 \to \chi\mu) \sim \frac{M_E^3}{64\pi v_\Phi^2} c_R^2 s_R^2 (1-x)^2, \tag{A35}$$

where $z \coloneqq m_{Z'}^2/M_E^2$ and $x \coloneqq m_\chi^2/M_E^2$. Hence the branching fraction of E_1, assuming no other decay modes, is approximately given by

$$\mathrm{BR}(E_1 \to Z'\mu) \sim \frac{(1-z)^2(1+2z)}{(1-z)^2(1+2z)+(1-x)^2}. \tag{A36}$$

At the benchmark point, $\mathrm{BR}(E_1 \to Z'\mu) \simeq 0.25$. The χ boson predominantly decays to VL fermions as far as these are kinematically allowed. If this is not the case, it should decay to a pair of SM leptons or quarks. For the lepton coupling, as seen from Eq. (A23), the coupling to 2 muons are strongly suppressed by the muon mass. Hence, the dominant decay mode of χ may be to a pair of top quarks due to the weaker suppression if $m_\chi > 2m_t$ which is true at the benchmark point. In this case, the processes with χ decays will not contribute to the $\mathrm{SRO}^{\mathrm{tight}}_{\mathrm{bveto}}$ and $\mathrm{SRO}^{\mathrm{loose}}_{\mathrm{bveto}}$ due to the b-jet veto, and thus the results in the main text will not be changed. If $m_\chi < 2m_t$, χ decays to a pair of bottom quarks, where the relevant Yukawa is estimated as $\sim\epsilon_{Q_3} m_b/M_Q \sim 10^{-4}$ for $\epsilon_{Q_3} \sim 0.1$ and $M_Q \sim 4$ TeV. This would be comparable to the decay to a pair of muons which the relevant Yukawa coupling is estimated as $\sim m_\mu/M_L \sim 10^{-4}$ for $M_L \sim 1$ TeV. Thus, there will be additional contributions with six muons on top of the decays from Z' boson.

[1] G. Aad *et al.* (ATLAS Collaboration), Observation of a new particle in the search for the Standard Model Higgs boson with the ATLAS detector at the LHC, Phys. Lett. B **716**, 1 (2012).

[2] S. Chatrchyan *et al.* (CMS Collaboration), Observation of a new boson at a mass of 125 GeV with the CMS Experiment at the LHC, Phys. Lett. B **716**, 30 (2012).

[3] R. Aaij *et al.* (LHCb Collaboration), Test of Lepton Universality Using $B^+ \to K^+\ell^+\ell^-$ Decays, Phys. Rev. Lett. **113**, 151601 (2014).

[4] R. Aaij *et al.* (LHCb Collaboration), Test of lepton universality with $B^0 \to K^{*0}\ell^+\ell^-$ decays, J. High Energy Phys. 08 (2017) 055.

[5] R. Aaij *et al.* (LHCb Collaboration), Search for Lepton-Universality Violation in $B^+ \to K^+\ell^+\ell^-$ Decays, Phys. Rev. Lett. **122**, 191801 (2019).

[6] A. Abdesselam *et al.* (Belle Collaboration), Test of Lepton Flavor Universality in $B \to K^*\ell^+\ell^-$ Decays at Belle, Phys. Rev. Lett. **126**, 161801 (2021).

[7] R. Aaij *et al.* (LHCb Collaboration), Differential branching fraction and angular analysis of the decay $B_s^0 \to \phi\mu^+\mu^-$, J. High Energy Phys. 07 (2013) 084.

[8] J. P. Lees *et al.* (*BABAR* Collaboration), Measurement of the $B \to X_s l^+ l^-$ Branching Fraction and Search for Direct *CP* Violation from a Sum of Exclusive Final States, Phys. Rev. Lett. **112**, 211802 (2014).

[9] R. Aaij *et al.* (LHCb Collaboration), Differential branching fractions and isospin asymmetries of $B \to K^{(*)}\mu^+\mu^-$ decays, J. High Energy Phys. 06 (2014) 133.

[10] R. Aaij *et al.* (LHCb Collaboration), Angular analysis and differential branching fraction of the decay $B_s^0 \to \phi\mu^+\mu^-$, J. High Energy Phys. 09 (2015) 179.

[11] R. Aaij *et al.* (LHCb Collaboration), Measurement of Form-Factor-Independent Observables in the Decay $B^0 \to K^{*0}\mu^+\mu^-$, Phys. Rev. Lett. **111**, 191801 (2013).

[12] V. Khachatryan *et al.* (CMS Collaboration), Angular analysis of the decay $B^0 \to K^{*0}\mu^+\mu^-$ from pp collisions at $\sqrt{s} = 8$ TeV, Phys. Lett. B **753**, 424 (2016).

[13] R. Aaij *et al.* (LHCb Collaboration), Angular analysis of the $B^0 \to K^{*0}\mu^+\mu^-$ decay using 3 fb^{-1} of integrated luminosity, J. High Energy Phys. 02 (2016) 104.

[14] A. Abdesselam *et al.* (Belle Collaboration), Angular analysis of $B^0 \to K^*(892)^0\ell^+\ell^-$, in *Proceedings, LHCSki 2016—A First Discussion of 13 TeV Results: Obergurgl, Austria, 2016* (2016).

[15] S. Wehle *et al.* (Belle Collaboration), Lepton-Flavor-Dependent Angular Analysis of $B \to K^*\ell^+\ell^-$, Phys. Rev. Lett. **118**, 111801 (2017).

[16] ATLAS Collaboration, Angular analysis of $B_d^0 \to K^* \mu^+ \mu^-$ decays in pp collisions at $\sqrt{s} = 8$ TeV with the ATLAS detector.

[17] CMS Collaboration, Measurement of the P_1 and P_5' angular parameters of the decay $B^0 \to K^{*0} \mu^+ \mu^-$ in proton-proton collisions at $\sqrt{s} = 8$ TeV.

[18] R. Aaij *et al.* (LHCb Collaboration), Angular Analysis of the $B^+ \to K^{*+} \mu^+ \mu^-$ Decay, Phys. Rev. Lett. **126**, 161802 (2021).

[19] R. Aaij *et al.* (LHCb Collaboration), Test of lepton universality in beauty-quark decays, arXiv:2103.11769.

[20] G. W. Bennett *et al.* (Muon g-2 Collaboration), Final report of the muon E821 anomalous magnetic moment measurement at BNL, Phys. Rev. D **73**, 072003 (2006).

[21] T. Aoyama *et al.*, The anomalous magnetic moment of the muon in the Standard Model, Phys. Rep. **887**, 1 (2020).

[22] B. Abi *et al.* (Muon g-2 Collaboration), Measurement of the Positive Muon Anomalous Magnetic Moment to 0.46 ppm, Phys. Rev. Lett. **126**, 141801 (2021).

[23] T. Aoyama, M. Hayakawa, T. Kinoshita, and M. Nio, Complete Tenth-Order QED Contribution to the Muon $g-2$, Phys. Rev. Lett. **109**, 111808 (2012).

[24] T. Aoyama, T. Kinoshita, and M. Nio, Theory of the anomalous magnetic moment of the electron, Atoms **7**, 28 (2019).

[25] A. Czarnecki, W. J. Marciano, and A. Vainshtein, Refinements in electroweak contributions to the muon anomalous magnetic moment, Phys. Rev. D **67**, 073006 (2003); **73**, 119901(E) (2006).

[26] C. Gnendiger, D. Stöckinger, and H. Stöckinger-Kim, The electroweak contributions to $(g-2)_\mu$ after the Higgs boson mass measurement, Phys. Rev. **88**, 053005 (2013).

[27] M. Davier, A. Hoecker, B. Malaescu, and Z. Zhang, Reevaluation of the hadronic vacuum polarisation contributions to the Standard Model predictions of the muon $g-2$ and $\alpha(m_Z^2)$ using newest hadronic cross-section data, Eur. Phys. J. C **77**, 827 (2017).

[28] A. Keshavarzi, D. Nomura, and T. Teubner, Muon $g-2$ and $\alpha(M_Z^2)$: A new data-based analysis, Phys. Rev. D **97**, 114025 (2018).

[29] G. Colangelo, M. Hoferichter, and P. Stoffer, Two-pion contribution to hadronic vacuum polarization, J. High Energy Phys. 02 (2019) 006.

[30] M. Hoferichter, B.-L. Hoid, and B. Kubis, Three-pion contribution to hadronic vacuum polarization, J. High Energy Phys. 08 (2019) 137.

[31] M. Davier, A. Hoecker, B. Malaescu, and Z. Zhang, A new evaluation of the hadronic vacuum polarisation contributions to the muon anomalous magnetic moment and to $\boldsymbol{\alpha(m_Z^2)}$, Eur. Phys. J. C **80**, 241 (2020); **80**, 410(E) (2020).

[32] A. Keshavarzi, D. Nomura, and T. Teubner, The $g-2$ of charged leptons, $\alpha(M_Z^2)$ and the hyperfine splitting of muonium, Phys. Rev. D **101**, 014029 (2020).

[33] A. Kurz, T. Liu, P. Marquard, and M. Steinhauser, Hadronic contribution to the muon anomalous magnetic moment to next-to-next-to-leading order, Phys. Lett. B **734**, 144 (2014).

[34] K. Melnikov and A. Vainshtein, Hadronic light-by-light scattering contribution to the muon anomalous magnetic moment revisited, Phys. Rev. D **70**, 113006 (2004).

[35] P. Masjuan and P. Sánchez-Puertas, Pseudoscalar-pole contribution to the $(g_\mu - 2)$: A rational approach, Phys. Rev. D **95**, 054026 (2017).

[36] G. Colangelo, M. Hoferichter, M. Procura, and P. Stoffer, Dispersion relation for hadronic light-by-light scattering: Two-pion contributions, J. High Energy Phys. 04 (2017) 161.

[37] M. Hoferichter, B.-L. Hoid, B. Kubis, S. Leupold, and S. P. Schneider, Dispersion relation for hadronic light-by-light scattering: Pion pole, J. High Energy Phys. 10 (2018) 141.

[38] A. Gérardin, H. B. Meyer, and A. Nyffeler, Lattice calculation of the pion transition form factor with $N_f = 2+1$ Wilson quarks, Phys. Rev. D **100**, 034520 (2019).

[39] J. Bijnens, N. Hermansson-Truedsson, and A. Rodríguez-Sánchez, Short-distance constraints for the HLbL contribution to the muon anomalous magnetic moment, Phys. Lett. B **798**, 134994 (2019).

[40] G. Colangelo, F. Hagelstein, M. Hoferichter, L. Laub, and P. Stoffer, Longitudinal short-distance constraints for the hadronic light-by-light contribution to $(g-2)_\mu$ with large-N_c Regge models, J. High Energy Phys. 03 (2020) 101.

[41] T. Blum, N. Christ, M. Hayakawa, T. Izubuchi, L. Jin, C. Jung, and C. Lehner, The Hadronic Light-By-Light Scattering Contribution to the Muon Anomalous Magnetic Moment from Lattice QCD, Phys. Rev. Lett. **124**, 132002 (2020).

[42] G. Colangelo, M. Hoferichter, A. Nyffeler, M. Passera, and P. Stoffer, Remarks on higher-order hadronic corrections to the muon $g-2$, Phys. Lett. B **735**, 90 (2014).

[43] J. Kawamura, S. Raby, and A. Trautner, Complete vectorlike fourth family and new U(1)' for muon anomalies, Phys. Rev. D **100**, 055030 (2019).

[44] J. Kawamura, S. Raby, and A. Trautner, Complete vectorlike fourth family with U(1)': A global analysis, Phys. Rev. D **101**, 035026 (2020).

[45] B. Allanach, F. S. Queiroz, A. Strumia, and S. Sun, Z' models for the LHCb and $g-2$ muon anomalies, Phys. Rev. D **93**, 055045 (2016); **95**, 119902(E) (2017).

[46] W. Altmannshofer, M. Carena, and A. Crivellin, $L_\mu - L_\tau$ theory of Higgs flavor violation and $(g-2)_\mu$, Phys. Rev. D **94**, 095026 (2016).

[47] E. Megias, M. Quiros, and L. Salas, $g_\mu - 2$ from vectorlike leptons in warped space, J. High Energy Phys. 05 (2017) 016.

[48] S. Raby and A. Trautner, Vectorlike chiral fourth family to explain muon anomalies, Phys. Rev. D **97**, 095006 (2018).

[49] S. F. King, Flavourful Z' models for $R_{K^{(*)}}$, J. High Energy Phys. 08 (2017) 019.

[50] L. Darmé, K. Kowalska, L. Roszkowski, and E. M. Sessolo, Flavor anomalies and dark matter in SUSY with an extra U(1), J. High Energy Phys. 10 (2018) 052.

[51] A. Czarnecki and W. J. Marciano, The muon anomalous magnetic moment: A Harbinger for "new physics", Phys. Rev. D **64**, 013014 (2001).

[52] K. Kannike, M. Raidal, D. M. Straub, and A. Strumia, Anthropic solution to the magnetic muon anomaly: The charged See-Saw, J. High Energy Phys. 02 (2012) 106; 10 (2012) 136(E).

[53] R. Dermisek and A. Raval, Explanation of the muon g-2 anomaly with vectorlike leptons and its implications for Higgs decays, Phys. Rev. D **88**, 013017 (2013).

[54] Z. Poh and S. Raby, Vectorlike leptons: Muon g-2 anomaly, lepton flavor violation, Higgs boson decays, and lepton nonuniversality, Phys. Rev. D **96**, 015032 (2017).

[55] A. Crivellin, M. Hoferichter, and P. Schmidt-Wellenburg, Combined explanations of $(g-2)_{\mu,e}$ and implications for a large muon EDM, Phys. Rev. D **98**, 113002 (2018).

[56] J. Kawamura, S. Okawa, and Y. Omura, Current status and muon $g-2$ explanation of lepton portal dark matter, J. High Energy Phys. 08 (2020) 042.

[57] Y. Bai and J. Berger, Muon g-2 in lepton portal dark matter, arXiv:2104.03301.

[58] A. Crivellin, F. Kirk, C. A. Manzari, and M. Montull, Global electroweak fit and vector-like leptons in light of the Cabibbo angle anomaly, J. High Energy Phys. 12 (2020) 166.

[59] B. Gripaios, M. Nardecchia, and S. A. Renner, Linear flavour violation and anomalies in B physics, J. High Energy Phys. 06 (2016) 083.

[60] P. Arnan, L. Hofer, F. Mescia, and A. Crivellin, Loop effects of heavy new scalars and fermions in $b \to s\mu^+\mu^-$, J. High Energy Phys. 04 (2017) 043.

[61] B. Grinstein, S. Pokorski, and G. G. Ross, Lepton nonuniversality in B decays and fermion mass structure, J. High Energy Phys. 12 (2018) 079.

[62] P. Arnan, A. Crivellin, M. Fedele, and F. Mescia, Generic loop effects of new scalars and fermions in $b \to s\ell^+\ell^-$ and a vector-like 4th generation, J. High Energy Phys. 06 (2019) 118.

[63] C.-W. Chiang and H. Okada, A simple model for explaining muon-related anomalies and dark matter, Int. J. Mod. Phys. A **34**, 1950106 (2019).

[64] J. M. Cline and J. M. Cornell, $R(K^{(*)})$ from dark matter exchange, Phys. Lett. B **782**, 232 (2018).

[65] J. Kawamura, S. Okawa, and Y. Omura, Interplay between the b $\to s\ell\ell$ anomalies and dark matter physics, Phys. Rev. D **96**, 075041 (2017).

[66] D. G. Cerdeño, A. Cheek, P. Martín-Ramiro, and J. M. Moreno, B anomalies and dark matter: A complex connection, Eur. Phys. J. C **79**, 517 (2019).

[67] G. Arcadi, L. Calibbi, M. Fedele, and F. Mescia, Muon $g-2$ and B-anomalies from Dark Matter, arXiv:2104.03228.

[68] G. Arcadi, L. Calibbi, M. Fedele, and F. Mescia, Systematic approach to B-physics anomalies and t-channel dark matter, arXiv:2103.09835.

[69] G. Aad *et al.* (ATLAS Collaboration), Search for supersymmetry in events with four or more charged leptons in 139 fb^{-1} of $\sqrt{s} = 13$ TeV pp collisions with the ATLAS detector, arXiv:2103.11684.

[70] A. J. Buras and M. Munz, Effective Hamiltonian for $B \to X(s)e^+e^-$ beyond leading logarithms in the NDR and HV schemes, Phys. Rev. D **52**, 186 (1995).

[71] C. Bobeth, M. Misiak, and J. Urban, Photonic penguins at two loops and m_t dependence of $BR[B \to X_s l^+ l^-]$, Nucl. Phys. **B574**, 291 (2000).

[72] G. Aad *et al.* (ATLAS Collaboration), Search for high-mass dilepton resonances using 139 fb^{-1} of pp collision data collected at $\sqrt{s} = 13$ TeV with the ATLAS detector, Phys. Lett. B **796**, 68 (2019).

[73] M. Kohda, T. Modak, and A. Soffer, Identifying a Z' behind $b \to s\ell\ell$ anomalies at the LHC, Phys. Rev. D **97**, 115019 (2018).

[74] B. C. Allanach, J. M. Butterworth, and T. Corbett, Collider constraints on z' models for neutral current B—anomalies, J. High Energy Phys. 08 (2019) 106.

[75] L.-S. Geng, B. Grinstein, S. Jäger, S.-Y. Li, J. M. Camalich, and R.-X. Shi, Implications of new evidence for lepton-universality violation in $b \to s\ell^+\ell^-$ decays, arXiv:2103.12738.

[76] W. Altmannshofer and P. Stangl, New physics in rare b decays after Moriond 2021, arXiv:2103.13370.

[77] A. Carvunis, F. Dettori, S. Gangal, D. Guadagnoli, and C. Normand, On the effective lifetime of $B_s \to \mu\mu\gamma$, arXiv:2102.13390.

[78] W. Altmannshofer, C. Niehoff, P. Stangl, and D. M. Straub, Status of the $B \to K^*\mu^+\mu^-$ anomaly after Moriond 2017, Eur. Phys. J. C **77**, 377 (2017).

[79] W. Altmannshofer, P. Stangl, and D. M. Straub, Interpreting hints for lepton flavor universality violation, Phys. Rev. D **96**, 055008 (2017).

[80] A. K. Alok, B. Bhattacharya, A. Datta, D. Kumar, J. Kumar, and D. London, New physics in $b \to s\mu^+\mu^-$ after the measurement of R_{K^*}, Phys. Rev. D **96**, 095009 (2017).

[81] B. Capdevila, A. Crivellin, S. Descotes-Genon, J. Matias, and J. Virto, Patterns of new physics in $b \to s\ell^+\ell^-$ transitions in the light of recent data, J. High Energy Phys. 01 (2018) 093.

[82] M. Ciuchini, A. M. Coutinho, M. Fedele, E. Franco, A. Paul, L. Silvestrini, and M. Valli, On flavourful easter eggs for new physics hunger and lepton flavour universality violation, Eur. Phys. J. C **77**, 688 (2017).

[83] G. D'Amico, M. Nardecchia, P. Panci, F. Sannino, A. Strumia, R. Torre, and A. Urbano, Flavour anomalies after the R_{K^*} measurement, J. High Energy Phys. 09 (2017) 010.

[84] L.-S. Geng, B. Grinstein, S. Jäger, J. M. Camalich, X.-L. Ren, and R.-X. Shi, Towards the discovery of new physics with lepton-universality ratios of $b \to s\ell\ell$ decays, Phys. Rev. D **96**, 093006 (2017).

[85] D. Ghosh, Explaining the R_K and R_{K^*} anomalies, Eur. Phys. J. C **77**, 694 (2017).

[86] A. Arbey, T. Hurth, F. Mahmoudi, and S. Neshatpour, Hadronic and new physics contributions to $b \to s$ transitions, Phys. Rev. D **98**, 095027 (2018).

[87] J. Aebischer, W. Altmannshofer, D. Guadagnoli, M. Reboud, P. Stangl, and D. M. Straub, B-decay discrepancies after Moriond 2019, Eur. Phys. J. C **80**, 252 (2020).

[88] M. Algueró, B. Capdevila, A. Crivellin, S. Descotes-Genon, P. Masjuan, J. Matias, M. N. Brunet, and J. Virto, Emerging patterns of new physics with and without lepton flavour universal contributions, Eur. Phys. J. C **79**, 714 (2019); **80**, 511(E) (2020).

[89] A. K. Alok, A. Dighe, S. Gangal, and D. Kumar, Continuing search for new physics in $b \to s\mu\mu$ decays: Two operators at a time, J. High Energy Phys. 06 (2019) 089.

[90] M. Ciuchini, A. M. Coutinho, M. Fedele, E. Franco, A. Paul, L. Silvestrini, and M. Valli, New physics in $b \to s\ell^+\ell^-$ confronts new data on lepton Universality, Eur. Phys. J. C **79**, 719 (2019).
[91] A. Datta, J. Kumar, and D. London, The B anomalies and new physics in $b \to se^+e^-$, Phys. Lett. B **797**, 134858 (2019).
[92] K. Kowalska, D. Kumar, and E. M. Sessolo, Implications for new physics in $b \to s\mu\mu$ transitions after recent measurements by Belle and LHCb, Eur. Phys. J. C **79**, 840 (2019).
[93] A. Arbey, T. Hurth, F. Mahmoudi, D. M. Santos, and S. Neshatpour, Update on the b → s anomalies, Phys. Rev. D **100**, 015045 (2019).
[94] D. Kumar, K. Kowalska, and E. M. Sessolo, Global Bayesian analysis of new physics in $b \to s\mu\mu$ transitions after Moriond-2019, 2019.
[95] G. Aad *et al.* (ATLAS Collaboration), Search for heavy lepton resonances decaying to a Z boson and a lepton in pp collisions at $\sqrt{s} = 8$ TeV with the ATLAS detector, J. High Energy Phys. 09 (2015) 108.
[96] R. Dermisek, J. P. Hall, E. Lunghi, and S. Shin, Limits on vectorlike leptons from searches for anomalous production of multi-lepton events, J. High Energy Phys. 12 (2014) 013.
[97] A. M. Sirunyan *et al.* (CMS Collaboration), Search for vector-like leptons in multilepton final states in proton-proton collisions at $\sqrt{s} = 13$ TeV, Phys. Rev. D **100**, 052003 (2019).
[98] N. Kumar and S. P. Martin, Vectorlike leptons at the large hadron collider, Phys. Rev. D **92**, 115018 (2015).
[99] A. Falkowski, D. M. Straub, and A. Vicente, Vector-like leptons: Higgs decays and collider phenomenology, J. High Energy Phys. 05 (2014) 092.
[100] S. A. R. Ellis, R. M. Godbole, S. Gopalakrishna, and J. D. Wells, Survey of vector-like fermion extensions of the Standard Model and their phenomenological implications, J. High Energy Phys. 09 (2014) 130.
[101] P. N. Bhattiprolu and S. P. Martin, Prospects for vectorlike leptons at future proton-proton colliders, Phys. Rev. D **100**, 015033 (2019).
[102] J. Ellis, TikZ-Feynman: Feynman diagrams with TikZ, Comput. Phys. Commun. **210**, 103 (2017).
[103] M. Dohse, TikZ-FeynHand: Basic user guide, arXiv:1802.00689.
[104] G. Aad *et al.* (ATLAS Collaboration), Search for electroweak production of charginos and sleptons decaying into final states with two leptons and missing transverse momentum in $\sqrt{s} = 13$ TeV pp collisions using the ATLAS detector, Eur. Phys. J. C **80**, 123 (2020).
[105] J. Alwall, R. Frederix, S. Frixione, V. Hirschi, F. Maltoni, O. Mattelaer, H. S. Shao, T. Stelzer, P. Torrielli, and M. Zaro, The automated computation of tree-level and next-to-leading order differential cross sections, and their matching to parton shower simulations, J. High Energy Phys. 07 (2014) 079.
[106] C. Degrande, C. Duhr, B. Fuks, D. Grellscheid, O. Mattelaer, and T. Reiter, UFO—The Universal FeynRules Output, Comput. Phys. Commun. **183**, 1201 (2012).
[107] N. D. Christensen and C. Duhr, FeynRules—Feynman rules made easy, Comput. Phys. Commun. **180**, 1614 (2009).
[108] J. de Favereau, C. Delaere, P. Demin, A. Giammanco, V. Lemaître, A. Mertens, and M. Selvaggi (DELPHES 3 Collaboration), DELPHES 3, A modular framework for fast simulation of a generic collider experiment, J. High Energy Phys. 02 (2014) 057.
[109] C. G. Lester and D. J. Summers, Measuring masses of semiinvisibly decaying particles pair produced at hadron colliders, Phys. Lett. B **463**, 99 (1999).
[110] A. Barr, C. Lester, and P. Stephens, m(T2): The truth behind the glamour, J. Phys. G **29**, 2343 (2003).
[111] C. G. Lester and B. Nachman, Bisection-based asymmetric M_{T2} computation: A higher precision calculator than existing symmetric methods, J. High Energy Phys. 03 (2015) 100.
[112] A. M. Sirunyan *et al.* (CMS Collaboration), Search for resonant and nonresonant new phenomena in high-mass dilepton final states at $\sqrt{s} = 13$ TeV, arXiv:2103.02708.
[113] P. N. Bhattiprolu, S. P. Martin, and J. D. Wells, Criteria for projected discovery and exclusion sensitivities of counting experiments, Eur. Phys. J. C **81**, 123 (2021).
[114] F. Jegerlehner and A. Nyffeler, The muon g-2, Phys. Rep. **477**, 1 (2009).
[115] W. Altmannshofer, S. Gori, M. Pospelov, and I. Yavin, Quark flavor transitions in $L_\mu - L_\tau$ models, Phys. Rev. D **89**, 095033 (2014).
[116] W. Altmannshofer, S. Gori, M. Pospelov, and I. Yavin, Neutrino Trident Production: A Powerful Probe of New Physics with Neutrino Beams, Phys. Rev. Lett. **113**, 091801 (2014).
[117] G. Magill and R. Plestid, Neutrino trident production at the intensity frontier, Phys. Rev. D **95**, 073004 (2017).
[118] S.-F. Ge, M. Lindner, and W. Rodejohann, Atmospheric trident production for probing new physics, Phys. Lett. B **772**, 164 (2017).
[119] P. Ballett, M. Hostert, S. Pascoli, Y. F. Perez-Gonzalez, Z. Tabrizi, and R. Z. Funchal, Neutrino trident scattering at near detectors, J. High Energy Phys. 01 (2019) 119.
[120] W. Altmannshofer, S. Gori, J. Martín-Albo, A. Sousa, and M. Wallbank, Neutrino tridents at DUNE, Phys. Rev. D **100**, 115029 (2019).